

STRUCTURE AND CATHODOLUMINESCENT PROPERTIES OF $Y_2O_3:Eu$ THIN FILMS AT DIFFERENT ACTIVATOR CONCENTRATIONS

O. M. Bordun,* I. O. Bordun, I. Yo. Kukharskyy,
Zh. Ya. Tsapovska, and M. V. Partyka

UDC 535.37:621.315.612;539.216.2

The surface structure and cathodoluminescence (CL) spectra of thin films of $Y_2O_3:Eu$ obtained by HF ion plasma sputtering were investigated by varying the activator concentration in the range of 1.0–7.5 mole%. The possibility of creating irregular solutions of yttrium and europium oxides and the structural features of the small and large crystallites that form the $Y_2O_3:Eu$ film were demonstrated on the basis of the shape of the CL spectra at different activator concentrations. The critical distance for interaction between the Eu^{3+} ions at nodes with C_2 and C_{3i} point symmetry was estimated, and a mechanism of energy migration between these centers was proposed.

Keywords: yttrium oxide, surface texture, cathodoluminescence, thin film.

Introduction. The interest in thin films of metal oxide materials arises from their potential use in optoelectronics and instrument manufacture. Such films and other materials doped with rare-earth ions (REIs) are key elements in modern devices for the generation, transmission, and control of optical signals. A special position among these materials is occupied by $Y_2O_3:Eu$, which has already passed the research stage and is regularly produced in the form of powdered cathodoluminophors. On account of the linear dependence of the brightness of emission on the density of the excitation current some manufacturers use only $Y_2O_3:Eu$ exclusively as red component of projection televisions and also in the creation of flat full-color vacuum fluorescent displays (VFDs) and field-emission displays (FEDs) [1–3].

A disadvantage of the material is the unsatisfactory morphology of the particles, which does not give smooth and uniform coverage of the screens or high resolving power. Such a situation has given rise to active study of various nanostructured objects based on $Y_2O_3:Eu$ [4–7]. It was noticed that a series of characteristics of the material change when the crystals reach nanometer sizes. These changes may be due both to quantum-size effects and to an increased role of various surface effects. A combination of small sizes for the crystalline particles and the presence of a doping additive [a luminescent center (Eu^{3+} ion)] ensures equilibrium coverage of the screen during deposition of thin films of $Y_2O_3:Eu$ consisting of nanocrystalline grains and efficient and stable luminescence and helps to extend the potential regions of application.

A whole series of methods have been used to produce films based on $Y_2O_3:Eu^{3+}$. As a result of the difference in their degree of perfection such films differ in optical and luminescent properties. For this reason in the present work the surface structure, spectral characteristics, and cathodoluminescent (CL) intensity of thin films of $Y_2O_3:Eu^{3+}$ produced by high-frequency (HF) ion plasma sputtering, depending on the concentration of the doping additive and the sizes of the crystallites, were investigated. We note that the HF ion plasma sputtering technique is the best method for the production of uniform semiconductor and dielectric films [8, 9].

Experimental. Thin films of $Y_2O_3:Eu$ with thickness of 0.2–1.0 μm were prepared by HF ion plasma sputtering in an atmosphere of 100% oxygen or 100% argon in a system with the magnetic field of external solenoids for compression and additional ionization of the plasma column on substrates of fused quartz v-SiO₂. The starting material was Y_2O_3 of ItO-I grade and Eu_2O_3 of special purity grade. The concentration of the activator was varied in the range of 1.0–7.5 mole%. After deposition of the films they were heat treated in air at 950–1050°C. The x-ray diffraction investigations showed the presence of a polycrystalline structure with preferred orientation in the (222) plane. The diffractograms were practically analogous with the diffractograms of pure films of Y_2O_3 [10]. In the $Y_2O_3:Eu$ films produced in an argon atmosphere the reflection from the (440) plane has somewhat higher intensity.

*To whom correspondence should be addressed.

TABLE 1. Surface Roughness of Films (R_a), Average Grain Diameters (a), Areas of Crystallites (S), and "Asymmetric Ratio" I_{612}/I_{596} in $Y_2O_3:Eu$ Thin Films

Eu ³⁺ , mole%	Production method	R_a , nm	a , nm	S , nm ²	I_{612}/I_{596}
1.0	Discrete evaporation	5.65	15.68	242	–
1.0	HF sputtering	5.31	15.86	307	8.56
2.5	HF sputtering	17.62	43.14	8027	9.25
5.0	HF sputtering	81.33	352.94	111,157	10.24
7.5	HF sputtering	–	–	–	11.37

The surface morphology of the films was investigated on a Russian Solver P47 PRO atomic-force microscope (AFM). The experimental data and the surface morphology parameters were processed with Image Analysis 2 software.

The CL characteristics were investigated in the pulsed electronic excitation mode. The spectra were recorded on apparatus based on an MDR-12 spectrometer (Russia) with an FEU-79 photomultiplier, the signal from which was delivered to a resonance amplifier and recorded by an ammeter and was also transmitted through an analog-digital converter to a PC to record the luminescence spectrum. The wavelengths were scanned by a monochromator using a stepping motor controlled by a computer through a control unit. The luminescence spectra were investigated in the region of 500–800 nm at 295 K.

Results and Discussion. Characteristic photomicrographs of the surface of $Y_2O_3:Eu$ films with equal concentration of activator, obtained by AFM, are presented in Figs. 1 and 2. As seen, the sizes of the crystalline grains and the roughness of the surface of the films are affected significantly by the concentration of the activator Eu^{3+} . Here the method of production has a smaller effect on the structural parameters of the film than the concentration of the activator (Fig. 1). Characteristic structural parameters of the surface of the $Y_2O_3:Eu$ films are presented in Table 1. The $Y_2O_3:Eu$ films obtained by ion plasma sputtering have somewhat larger sizes for the crystalline grains than with discrete deposition although they are characterized by lower surface roughness. Here increase of the concentration of the Eu^{3+} activator leads to substantial increase both in the sizes of the crystallites and in the roughness of the surface relief of the $Y_2O_3:Eu$ films (Fig. 2).

Investigation of the CL spectra of $Y_2O_3:Eu$ thin films with various activator concentrations shows (Fig. 3) that the form of the spectra does not change, at least during variation of the concentration of the activator in the region of 1.0–7.5 mole%. The spectra contain narrow bands arising from intra-center transitions between the electron shells of the activator Eu^{3+} and associated with the permitted ${}^5D_0-{}^7F_1$ magnetic dipole transitions (for the Eu^{3+} ions at the C_2 and C_{3i} points of the $Y_2O_3:Eu$ crystal lattice) and the permitted ${}^5D_0-{}^7F_2$ electric dipole transitions (only for the Eu^{3+} ions at the C_2 points) [11, 12]. In addition, it was established that the $Y_2O_3:Eu$ films deposited in both argon and of oxygen atmospheres have a maximum CL yield at an activator content of 5.0 mole% (Fig. 3, inset). At lower concentrations the sizes of the crystalline grains are smaller, which increases the relative contribution from grain-boundary scattering. At larger activator concentrations concentration quenching is probably observed as a result of the creation of a more defective structure and of increase in the number of channels for nonradiative relaxation. Increase of the activator concentration can also increase the diffusion of Eu^{3+} ions into the nodes of Y_2O_3 crystal lattice with C_{3i} point symmetry, for which electric dipole radiation is forbidden by the selection rules.

The so-called "asymmetric ratio" I_{612}/I_{596} of the intensities of the luminescence maxima at 612 and 596 nm, which corresponds to the ratio of the number of Eu^{3+} cations in the local symmetry states N_{C2}/N_{C3i} , is often used in description of the luminescence spectrum of Y_2O_3 [6, 13–15]. The band with a maximum at 612 nm is determined by the electric dipole transition ${}^5D_0-{}^7F_2$, which is very sensitive to the nearest environment of the emitting Eu^{3+} ion. The band with a maximum at 596 nm is determined by the magnetic dipole ${}^5D_0-{}^7F_1$ transition, which is not sensitive to the nearest environment [15–18]. The ratio of the amplitude intensities I_{612}/I_{596} is used to estimate N_{C2}/N_{C3i} [6, 13–15] and analyze the structural perfection of $Y_2O_3:Eu$.

For Y^{3+} ions in the Y_2O_3 matrix in the equilibrium state in the ideal lattice $N_{C2}/N_{C3i} = 3:1$ [19]. A similar result must be obtained during equilibrium substitution of Y^{3+} ions by Eu^{3+} ions. However, the ratio is much larger in thin films of $Y_2O_3:Eu$ and depends on the concentration of the activating impurity. In particular, increase of the concentration of Eu^{3+} from 1.0 to 7.5 mole % leads to increase of N_{C2}/N_{C3i} from 8.56 to 11.37 (Table 1). We note that fairly close results for the amplitude ratio $I_{612}/I_{596} = 8-10$ were obtained in [13] during investigation of the photoluminescence of powdered

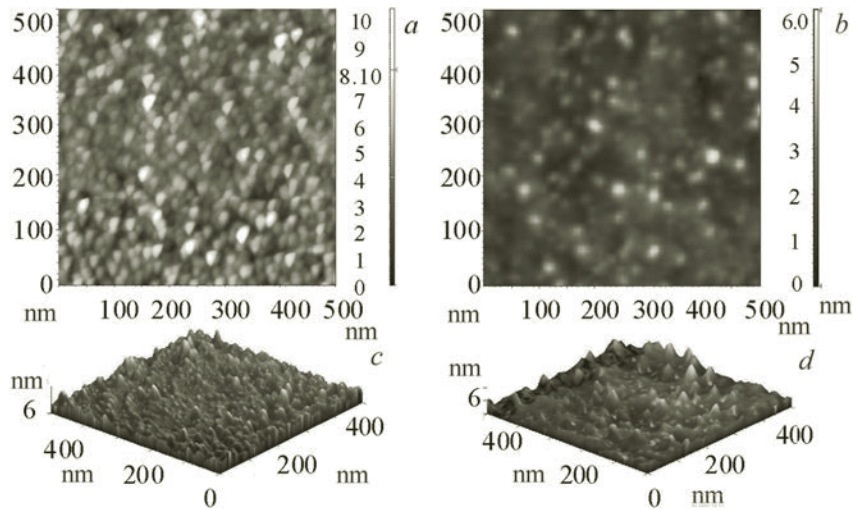


Fig. 1. Image of the surface morphology of $Y_2O_3:Eu$ thin films obtained by discrete evaporation (a, c) and HF ion plasma sputtering in an argon atmosphere (b, d) with activator concentration of 1 mole%.

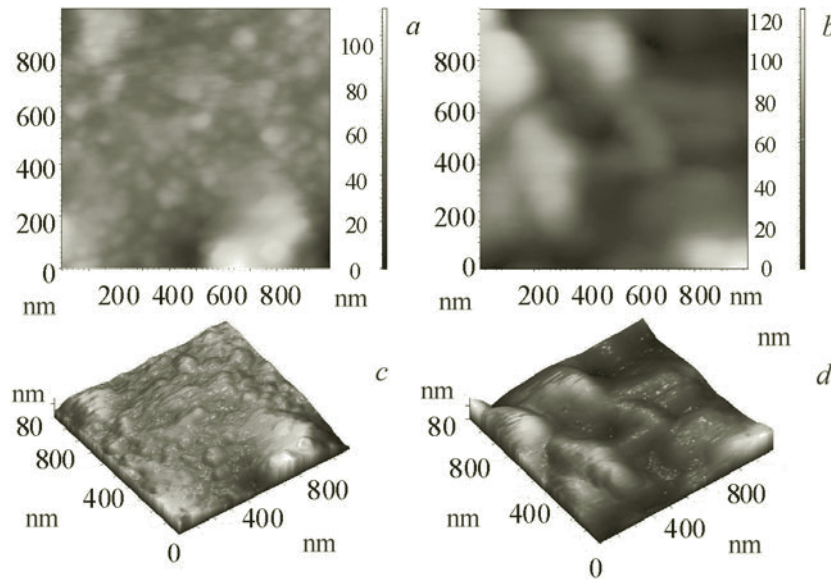


Fig. 2. Image of the surface morphology of $Y_2O_3:Eu$ thin films obtained by HF ion plasma sputtering in an argon atmosphere with activator concentrations of 2.5 (a, c) and 5 mole% (b, d).

$Y_2O_3:Eu$ materials with various degrees of dispersion obtained by the sol-gel method. Investigation of the “asymmetric ratio” during the photoluminescence of $Y_2O_3:Eu$ nanoparticles, to which the emission of our crystallites of corresponding dimensions can be assigned, shows that its value depends on the size of the nanoparticles and increases from 9.53 to 10.45 with increase of the sizes of the $Y_2O_3:Eu$ nanocrystals from 8.5 to 53.5 nm [20]. According to [7], during hydrolysis deposition of $Y_2O_3:Eu$ nanoparticles increase in the concentration of the activator from 1.0 to 5.0 mole% leads to increase of the size of the nanoparticles from 10 to 16 nm during annealing at 600°C and from 20 to 25 nm during annealing at 900°C. Here the I_{612}/I_{596} ratio depends on the excitation wavelength: at $\lambda_{exc} = 410$ nm it increases from 10.44 to 10.91 with change in the concentration of the activator from 1.0 to 5.9 mole% and at $\lambda_{exc} = 532$ nm it increases from 10.34 to 11.54.

The data that we obtained agree with the results of other investigations of $Y_2O_3:Eu$ nanoparticles and indicate that the sizes of the crystalline grains in the $Y_2O_3:Eu$ film increase with increase of the activator concentration and in CL the relative contribution from emission of the Eu^{3+} ions at the nodes in C_2 point symmetry increases in relation to the nodes

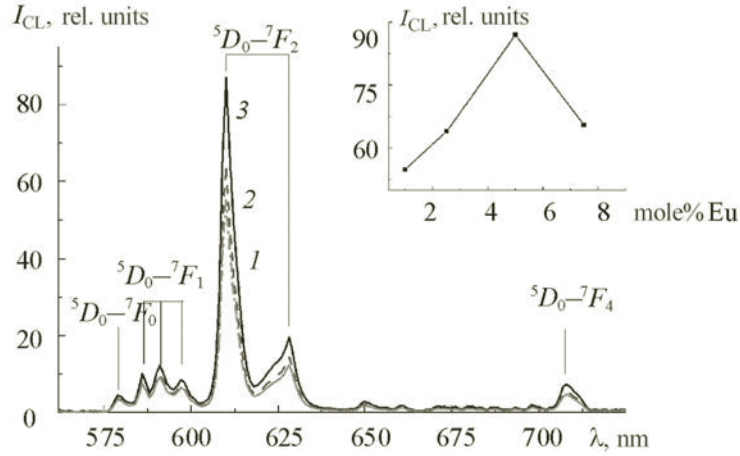


Fig. 3. The CL spectra of $Y_2O_3:Eu$ thin films with activator concentrations of 1 (1), 2.5 (2), and 5 mole% (3) (half-width of recording band <1.5 nm). Parameters of electron irradiation pulses: current density of electron beam $j = 5 \cdot 10^{-2}$ A/m²; length of pulses $5 \cdot 10^{-4}$ s; pause between pulses 0.1 s; energy of exciting electrons 5 keV. Inset: dependence of the intensity of the $^5D_0-^7F_2$ transition in the CL spectra of $Y_2O_3:Eu$ thin films on the activator concentration.

with C_{3i} point symmetry (Fig. 3). Such deviation most likely indicates possible creation of irregular solutions of yttrium and europium oxide in the thin film of $Y_2O_3:Eu$ during deposition and annealing. The increase of the relative amount of Eu^{3+} ions at the C_2 position in crystallites of larger dimensions is due to reduction of the local symmetry in the environment of the europium ions by the oxygen ions. Since the film was annealed in air, in the annealing process the local symmetry of the Eu^{3+} ions was mostly increased close to the surface. Such surface effects are of course more perceptible in crystallites of smaller dimensions since their contribution in the observed luminescence spectra is more substantial.

Figure 4 shows the dependence of I_{612}/I_{596} on the concentration of the activator Eu^{3+} in thin films of $Y_2O_3:Eu$ and on the average distance between the Eu^{3+} ions in the $Y_2O_3:Eu$ lattice. This average distance for a cubic lattice is determined according to [21] by:

$$D_{Eu} = \sqrt[3]{\frac{100M}{2\rho N_A C}}, \quad (1)$$

where M is the molecular mass of Y_2O_3 ; $\rho = 5.10$ g/cm³ is the density of Y_2O_3 ; N_A is Avogadro's number; C is concentration, %. According to Eq. (1), the average distance between Eu^{3+} at the nodes with point symmetry C_2 and C_{3i} is a function of the concentration of the activator.

If all the Y^{3+} ions in the Y_2O_3 lattice are substituted by Eu^{3+} ions the average distance between the Eu^{3+} ions, according to Eq. (1), amounts to 0.334 nm. In the Y_2O_3 lattice the shortest distance between the cations at the C_2 and C_{3i} nodes is 0.352 nm [22]. Comparison of these values shows that Eq. (1) represents the average distance between the Eu^{3+} ions at nodes with point symmetries C_2 and C_{3i} fairly well as a function of the concentration of Eu^{3+} .

Starting from [21], the I_{612}/I_{596} ratio as a function of the concentration C and the average distance between the ions of the activator D_{Eu} is given by the phenomenological equations:

$$I_{612}/I_{596} = G + H_1 C^\delta, \quad (2)$$

$$I_{612}/I_{596} = G + H_2 D_{Eu}^{-3\delta}, \quad (3)$$

where the parameters G and δ have identical values. The calculations show that in the investigated films $G = 7.93$, $H_1 = 0.63$, $H_2 = 54.8$, and $\delta = 0.81$.

Since the curvature of the approximation relationship in Fig. 4b for Eq. (3) is greater than in Fig. 4a it is possible from this relationship to obtain the inflection point more accurately, which for us was at 2.85 nm. This means that the critical distance D_{Eu} for the interaction between Eu^{3+} and the nodes with point symmetry C_2 and C_{3i} amounts to 2.85 nm.

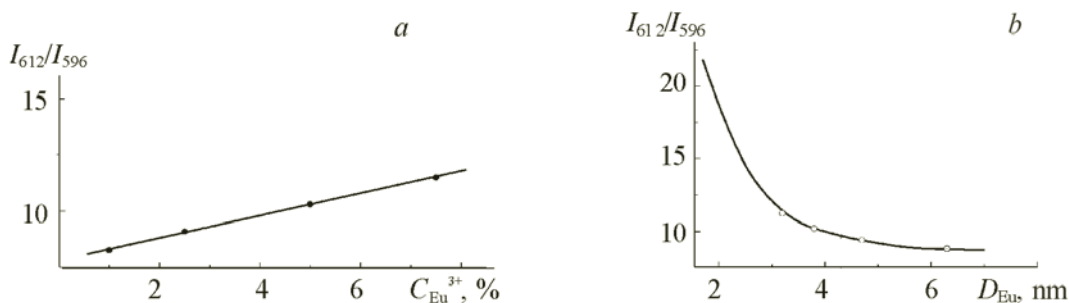


Fig. 4. Dependence of the intensity ratio I_{612}/I_{596} in the CL spectra of $Y_2O_3:Eu$ thin films on the concentration of the activator Eu^{3+} (a) and on the average distance between the Eu^{3+} ions in $Y_2O_3:Eu$ thin films (b).

The parameter R_0 , which characterizes the critical distance of energy transfer between the Eu^{3+} ions at positions C_2 and C_{3i} during radiative dissociation, was determined in a series of papers. For Eu^{3+} ions in cubic Y_2O_3 $R_0 = 0.87$ [21], 0.82 [23], and 0.86 nm [24], which is more than twice as large as the distance between the Eu^{3+} ions at positions C_2 and C_{3i} . However, if two spheres with radius R_0 are constructed for the Eu^{3+} ions at the nodes of the Y_2O_3 crystal lattice with point symmetry C_2 and C_{3i} it is seen that these spheres do not overlap for the critical distance $D_{Eu} = 2.85$ nm that we determined.

As follows from the results in [24], for the Eu^{3+} cations in $Y_2O_3:Eu$ at 8 K the diffusion length of migration $L = 2.4$ nm. The distance L of course increases with increase of temperature. On this basis the value of 2.85 nm that we obtained is less than the total distance ($L + R_0$). Such a situation most likely indicates that the transfer of energy between the C_2 and C_{3i} centers is realized not as a result of direct interaction of the centers but by diffusion migration involving the energy states of the Y_2O_3 crystal lattice. This is confirmed by the fact that the films annealed in various atmospheres have different structural perfection and, accordingly, different luminescence intensity. Here, the strongest emission is characteristic of the most perfect films of $Y_2O_3:Eu$ annealed in an atmosphere of argon [10].

Conclusions. It was shown that increase of the activator concentration during high-frequency ion plasma deposition of thin films of $Y_2O_3:Eu$ in the range of 1.0–5.0 mole% leads to substantial increase of the sizes of the crystallites forming the film (from 15.86 to 352.94 nm). The maximum cathodoluminescence yield in the investigated films deposited in an atmosphere of argon and oxygen is observed at an activator concentration of 5 mole%. It was established by analysis of the form of the cathodoluminescence spectra that the relative contribution from emission of the Eu^{3+} ions at the nodes of the Y_2O_3 crystal lattice with point symmetry C_2 in relation to the nodes with to point symmetry C_{3i} increases with increase of the activator concentration in cathodoluminescence. By determination of the critical distance for interaction between the Eu^{3+} ions at the nodes with point symmetry C_2 and C_{3i} it was suggested that energy transfer between these centers in $Y_2O_3:Eu$ thin films is realized by diffusion migration involving the energy states of the crystal lattice of the Y_2O_3 matrix.

REFERENCES

1. N. Yamamoto, *Cathodoluminescence*, Croatia, InTech (2012).
2. A. S. Bugaev, V. B. Kireev, E. P. Sheshin, and A. Yu. Kolodyazhnyi, *Usp. Fiz. Nauk*, **185**, No. 8, 853–883 (2015).
3. S. H. Cho, S. H. Know, J. S. Yoo, C. W. Oh, J. D. Lee, K. J. Hong, and S. J. Kwone, *J. Electrochem. Soc.*, **147**, No. 8, 3143–3147 (2000).
4. Q. Dai, M. E. Foley, C. J. Breshike, A. Lita, and G. F. Strouse, *J. Am. Chem. Soc.*, **133**, No. 39, 15475–15486 (2011).
5. C. Shanga, X. Shang, Y. Qu, and M. Li, *Chem. Phys. Lett.*, **501**, Nos. 4–6, 480–484 (2011).
6. R. Srinivasan, N. R. Yogamalar, J. Elanchezhian, R. J. Joseyphus, and A. C. Bose, *J. Alloys Compd.*, **496**, Nos. 1–2, 472–477 (2010).
7. P. Packiyaraj and P. Thangadurai, *J. Lumin.*, **145**, 997–1003 (2014).
8. L. Maissel and R. Glanga (Eds.), *Technology of Thin Films* [in Russian], Sov. Radio, Moscow (1977).
9. E. V. Berlin, and L. A. Seidman, *Ion Plasma Processes in Thin-Film Technology* [in Russian], Tekhnosfera, Moscow (2010).
10. O. M. Bordun, I. O. Bordun, and I. I. Kukharskii, *Zh. Prikl. Spektrosk.*, **82**, No. 3, 380–385 (2015) [O. M. Bordun, I. O. Bordun, and I. Yo. Kukharskyy, *J. Appl. Spectrosc.*, **82**, No. 3, 390–395 (2015)].

11. N. C. Chang and J. B. Gruber, *J. Chem. Phys.*, **41**, No. 10, 3227–3234 (1964).
12. G. Blasse and B. C. Grabmaier, *Luminescent Materials*, Springer-Verlag, Berlin (1994).
13. T. A. Pomelova, V. V. Bakovets, I. V. Korol'kov, O. V. Antonova, and I. P. Dolgovesova, *FTT*, **56**, No. 12, 2410–2419 (2014).
14. R. M. Krsmanović, Ž. Antić, M. G. Nikolić, M. Mitrić, and M. D. Dramićanin, *Ceram. Int.*, **37**, No. 2, 525–531 (2011).
15. H. Shi, X.-Y. Zhang, W.-L. Dong, X.-Y. Mi, N.-L. Wang, Y. Li, and H.-W. Liu, *Chin. Phys. B*, **25**, No. 4, 047802 (1–5) (2016).
16. S. Som, S. K. Sharma, and S. P. Lochab, *Mater. Res. Bull.*, **48**, No. 2, 844–851 (2013).
17. F. C. Romo, A. G. Murillo, D. L. Torres, N. C. Castro, V. H. Romero, E. Rosa, V. G. Febles, and M. G. Hernández, *Opt. Mater.*, **32**, No. 11, 1471–1479 (2010).
18. G. S. Gowd, M. K. Patra, S. Songara, A. Shukla, M. Mathew, S. R. Vadera, and N. Kumar, *J. Lumin.*, **132**, No. 8, 76–82 (2012).
19. F. Hanic, M. Hartmanova, S. Bagdasarov, G. G. Knab, and A. A. Urusovskaja, *Acta Crystallogr. B*, **40**, No. 2, 1723–1730 (1984).
20. W.-N. Wang, W. Widiyastuti, T. Ogi, I. W. Lenggoro, and K. Okuyama, *Chem. Mater.*, **19**, No. 7, 1723–1730 (2007).
21. D. den Engelsen, P. Harris, T. Ireland, and J. Silver, *ECS J. Sol. State Sci. Tech.*, **4**, No. 2, R1–R9 (2015).
22. J. Heber, K. H. Hellwege, U. Köbler, and H. Muzmann, *Z. Physik*, **237**, No. 3, 189–204 (1970).
23. M. Buijs, A. Meyerink, and G. Blasse, *J. Lumin.*, **37**, No. 1, 9–20 (1987).
24. S. Qiang, C. Barthou, J. P. Denis, F. Pelle, and B. Blanzat, *J. Lumin.*, **28**, No. 1, 1–11 (1983).